Quasiparticle lifetimes in magnesium clusters modeled by self-consistent GW# calculations

Citation: He, Yi, and Taofang Zeng. "Quasiparticle lifetimes in magnesium clusters modeled by self-consistent GWΓ calculations." Physical Review B 84 (2011): n. pag. Web. 17 Nov. 2011. © 2011 American Physical Society

As Published: http://dx.doi.org/10.1103/PhysRevB.84.035456

Publisher: American Physical Society

Persistent URL: http://hdl.handle.net/1721.1/67054

Version: Final published version: final published article, as it appeared in a journal, conference proceedings, or other formally published context

Quasiparticle lifetimes in magnesium clusters modeled by self-consistent $GW\Gamma$ calculations

Yi He and Taofang Zeng*

Department of Mechanical Engineering, Massachusetts Institute of Technology, 77 Massachusetts Avenue, Cambridge, Massachusetts 02139, USA

(Received 17 February 2011; published 29 July 2011)

Quasiparticle (QP) lifetimes in magnesium clusters are calculated using many-body Green's-function theory. We analyze the effect of the self-consistency of the one-particle Green's function G on the calculations and demonstrate the necessity of the implementation of such a self-consistency. Based on hot-electron and hot-hole lifetimes in Mg_{40} calculated by the $GW\Gamma$ method, we find that in the low-energy excitation regime, the QP lifetimes are longer than those in the free-electron gas with the electron density $r_s = 2.66$ ($3s^2$ of the bulk Mg) due to the lack of states available for transitions. In the high-excitation-energy regime, scaled lifetimes of hot electrons converge to the range of 21–24 fs eV^2. Scaled lifetimes of hot holes in this regime are shorter than those of hot electrons and decrease slightly with increasing excitation energies.

DOI: 10.1103/PhysRevB.84.035456 PACS number(s): 36.40.Cg, 73.22.−f

I. INTRODUCTION

Inelastic electron relaxation in materials is a phenomenon technically and fundamentally important in many physical and chemical processes.[1] The lifetimes of hot electrons (holes) in bulk metals and metallic surfaces have been widely investigated both experimentally and theoretically for several decades.[2–7] As a low-dimensional form of metals, metallic clusters demonstrate electronic structures distinct from their bulk counterparts.[8] This fact hence raises the question whether the dynamics of the electrons in a confined system is different from the bulk, which is important in nanoelectronics and photochemistry.[9,10] Yet the understanding about the inelastic electron-scattering processes in metallic clusters is still quite limited.

It is known that confined systems exhibit discrete electronic levels, possessing fewer states available for the transition of electrons, and thus hot electrons may have longer lifetimes as compared to electrons in the bulk. On the other hand, the screening effect is weakened in small metallic clusters due to the lack of electrons, increasing the scattering rate of electrons and reducing electrons lifetimes. Therefore the lifetime of a hot electron in a cluster can be either longer or shorter than that in corresponding bulk materials due to the two competing factors.[6]

Experimentally, time-resolved two-photon photoemission (TR2PPES) has been applied to measure the electronic lifetimes in metallic nanoparticles and clusters.[11–16] Measurements for internal electron thermalization times in silver nanoparticles embedded in a matrix show that the electron relaxation rate increases with decreasing particle size when the particle radius is less than 5 nm.[11] However, interferometric TR2PPES measurements for silver nanoparticles on graphite show that inelastic electron lifetimes are longer than those of a silver film.[12] The inconsistency for these experiments could be attributed to the following reasons. First, the electronic levels of the matrix may couple with those of the clusters embedded, and the screening due to the matrix can also affect the electronic lifetimes. Second, the first photon in the TR2PPES measurements intended for the single-particle excitation may also excite collective modes and complicate the electron scattering.

The quasiparticle (QP) lifetimes could be understood by using the state-of-the-art theory or computation. Many-body perturbation-theory-based GW method has been proven to be a powerful approach for the investigation of QP energies and lifetimes of bulk materials and surfaces.[17–20] Recently, the method has also been applied to the ideal jellium model, and it was found that the hot-electron lifetimes in nanoparticles are in the femtosecond time scale.[21] In this paper, we simulate inelastic lifetimes of electrons and holes in two Mg clusters for the understanding of the electronic dynamics in real metallic clusters.

II. METHODOLOGY

A. GW implementations

The damping rate of a hot electron or a hot hole due to the inelastic electron-electron scattering is evaluated as[22]

$$\tau_i^{-1} = 2|\mathrm{Im}\langle\psi_i|\Sigma_{\mathrm{xc}}(\mathbf{r},\mathbf{r}';E_i)|\psi_i\rangle|, \tag{1}$$

where τ_i, E_i, and ψ_i are the lifetime, energy, and wave function of the ith QP, respectively, and $\Sigma_{\mathrm{xc}}(\mathbf{r},\mathbf{r}';E_i)$ is the exchange-correlation self-energy operator in the QP equation:

$$(T + V_{\mathrm{ext}} + V_{\mathrm{H}})\psi_i(\mathbf{r}) + \int d\mathbf{r}'\Sigma_{\mathrm{xc}}(\mathbf{r},\mathbf{r}';E_i)\psi_i(\mathbf{r}') = E_i\psi_i(\mathbf{r}). \tag{2}$$

By following Hedin's scheme,[23] $\Sigma_{xc} = iGW\Gamma$ (with $\hbar = 1$), where Γ is the vertex function and G is the one-particle Green's function:

$$G(\mathbf{r},\mathbf{r}';E) = \sum_n \frac{\psi_n(\mathbf{r})\psi_n(\mathbf{r}')}{E - E_n + i\eta_n 0^+}, \tag{3}$$

where E_n are QP energies. W is the screened Coulomb interaction and can be obtained by solving the equation $W = V + VPW$, where V is the Coulomb interaction and $P = -iGG\Gamma$ is the irreducible polarizability. Both Σ_{xc} and P include the vertex function Γ. It has been shown that a consistent choice of Γ is necessary for the QP calculation.[24] A straightforward strategy is to approximate $\Gamma(1,2;3)$ with $\delta(1,3)\delta(2,3)$, which corresponds to the random phase approximation (RPA) for W and GW approximation (GWA)

for Σ_{xc}. An alternative method is to simplify the equation $\Gamma = 1 + (\partial\Sigma^0/\partial G)GG\Gamma$ by taking $\Sigma^0(1,2)$ as $V_{xc}(1)\delta(1,2)$ in the framework of the local density approximation (LDA), which is equivalent to the time-dependent LDA (TDLDA) for W and $GW\Gamma$ for Σ_{xc}. More details can be found in Refs. 25 and 26. In this study, both the RPA-GWA and the TDLDA-$GW\Gamma$ have been performed for the calculations of QP energies and lifetimes in Mg_{10} and Mg_{40}.

In the QP calculations of finite systems there are always some "pseudobound" states, whose energies are negative when calculated by density functional theory (DFT) but positive in the QP calculation. These states will relax to free-electron states in a full diagonalization QP calculation when a complete basis set is used.[27] Our QP calculations, on the other hand, focus on the truly bound states with negative QP energies; thus the QP wave functions are expected to be close to the DFT ones, and the off-diagonal elements $\langle\psi_i|\Sigma_{xc}|\psi_{i'}\rangle$ can be neglected. Then the QP equation can be solved as a perturbation to the DFT equation

$$\langle\psi_i|\Sigma_{xc}(\mathbf{r},\mathbf{r}';E_i)|\psi_i\rangle - \langle\psi_i|V_{xc}(\mathbf{r})|\psi_i\rangle = E_i - \epsilon_i, \quad (4)$$

where ϵ_i are the DFT eigenvalues. $\langle\psi_i|\Sigma_{xc}|\psi_i\rangle$ can be separated as an energy-independent exchange part $\langle\psi_i|\Sigma_x|\psi_i\rangle$ and an energy-dependent correlation part $\langle\psi_i|\Sigma_c|\psi_i\rangle$. To evaluate the latter one, we assume that the response of the density to the external potential, namely, the reducible polarizability $\Pi(\mathbf{r},\mathbf{r}';E)$, can be expressed as the summation of electron-hole excitation modes:[28]

$$\Pi(\mathbf{r},\mathbf{r}';E) = 2\sum_s \rho_s(\mathbf{r})\rho_s^*(\mathbf{r}') \times\left[\frac{1}{E-(\omega_s - i0^+)} - \frac{1}{E+(\omega_s - i0^+)}\right], \quad (5)$$

where

$$\rho_s(\mathbf{r}) = \sum_{v,c} R_s^{v,c}\psi_v^*(\mathbf{r})\psi_c(\mathbf{r}). \quad (6)$$

The eigenvectors $\mathbf{R}_s$ and eigenvalues ω_s are determined through the RPA or the TDLDA. Then $\Sigma_c(\mathbf{r},\mathbf{r}';E)$ is expressed as Eq. (7a) for the GWA or Eq. (7b) for the $GW\Gamma$:[29]

$$\Sigma_c(E) = i\int\frac{dE'}{2\pi}e^{-iE'0^+}G(E-E')V\Pi(E')V, \quad (7a)$$

$$\Sigma_c(E) = i\int\frac{dE'}{2\pi}e^{-iE'0^+}G(E-E')(V+f_{xc})\Pi(E')V. \quad (7b)$$

In Eq. (7b), $(V + f_{xc})\Pi(E')V$ is not written in Hermitian form since we only take into account the diagonal elements. By sandwiching $\Sigma_c(\mathbf{r},\mathbf{r}';E)$ with ψ_i, the energy-dependent correlation energy $\langle\psi_i|\Sigma_c|\psi_i\rangle$ can be evaluated as

$$\langle\psi_i|\Sigma_c|\psi_i\rangle = \sum_n\sum_s\frac{a_{n,s,i}}{E-E_n-\omega_s\eta_s}, \quad (8)$$

where $a_{n,s,i}$ equals $2\langle\psi_i\psi_n|V|\rho_s\rangle\langle\rho_s|V|\psi_i\psi_n\rangle$ for the GWA and $2\langle\psi_i\psi_n|(V+f_{xc})|\rho_s\rangle\langle\rho_s|V|\psi_i\psi_n\rangle$ for the $GW\Gamma$. The coefficient η_n is $+1$ for unoccupied states and -1 for occupied states, and E_n in the denominators are the QP energies introduced from the one-particle Green's function in Eq. (3).

B. Numerical details

The ground-state LDA calculations are performed using the SIESTA code.[30] Core electrons $[1s^22s^22p^6]$ of Mg are replaced by the nonlocal norm-conserving pseudopotential based on the Troullier-Martins scheme.[31] A double-ζ polarization (DZP) basis set of numerical atomic orbitals is used for the valance electrons of Mg. The cutoff radii are 10 a.u. for both s and p orbitals. The structures are optimized by simulated annealing using molecular dynamics with an exponential cooling schedule, followed by the conjugated gradient algorithm with the maximum force tolerance of 0.01 eV/Å. The optimized structures of Mg_{10} and Mg_{40} are illustrated in Fig. 1.

All integrals are evaluated on a uniform grid in real space with a grid spacing of 0.6 a.u., which has been tested to give QP energies with an accuracy of 0.1 eV. The exchange integrals $\int d\mathbf{r}\int d\mathbf{r}'\psi_i(\mathbf{r})\psi_j(\mathbf{r})V(\mathbf{r},\mathbf{r}')\psi_k(\mathbf{r}')\psi_l(\mathbf{r}')$ are evaluated by solving Poisson equations first with the multigrid method.[32] The convergence of the QP calculation usually requires a large number of unoccupied states for the evaluation of the polarizability. Thus a Coulomb-hole screened-exchange (COHSEX) remainder scheme has been applied to accelerate the convergence of the correlation part $\langle\psi_i|\Sigma_c|\psi_i\rangle$.[29] To obtain the imaginary parts of the system, analytical continuation is applied to extend Σ_c to the complex plane, and the complex QP energy $E_i - i\eta_i\gamma_i$ is calculated by solving a complex equation set numerically:

$$\mathrm{Re}\langle\psi_i|\Sigma_{xc}(E_i - i\eta_i\gamma_i)|\psi_i\rangle - \langle\psi_i|V_{xc}|\psi_i\rangle = E_i - \epsilon_i, \quad (9a)$$

$$\mathrm{Im}|\langle\psi_i|\Sigma_{xc}(E_i - i\eta_i\gamma_i)|\psi_i\rangle| = \gamma_i. \quad (9b)$$

III. RESULTS AND DISCUSSIONS

A. Effects of self-consistency on QP energies and lifetimes

In the QP calculations, a ready starting point is the approximation for G:

$$G(\mathbf{r},\mathbf{r}';E) \approx G_0(\mathbf{r},\mathbf{r}';E) = \sum_n\frac{\psi_n(\mathbf{r})\psi_n(\mathbf{r}')}{E-\epsilon_n+i\eta_n0^+}. \quad (10)$$

From G_0 we can calculate W_0 and thus Σ_{xc} and the QP energies E_n. However, introduction of Eq. (10) brings an uncertainty: whether we should recalculate every quantity with the updated G until its convergence, namely, self-consistency. It has been shown that the self-consistency cycles including W ($G\to W\to\Sigma_{xc}\to G$) may deteriorate the agreements

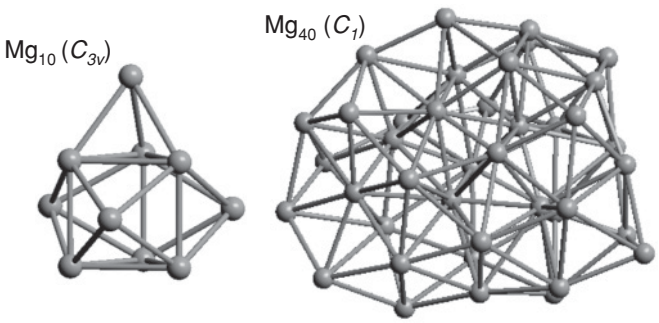

FIG. 1. Optimized structures of Mg_{10} and Mg_{40}. The labels in brackets correspond to the point-group symmetries of the clusters.

between the simulated results and experimental data.[33] So in this study, we take $W \equiv W_0$ and focus on the effect of self-consistency of G ($G \rightarrow \Sigma_{xc} \rightarrow G$) on the QP properties. For comparison, we solve Eq. (9)) only once in the non-self-consistent calculation. In the self-consistent calculation, however, G is updated after each cycle until its convergence. We speculate the self-consistency for the calculations of the QP lifetimes as follows.

The decay rate of the ith QP can be written as a summation $S_i = 2|\sum_n \sum_s \frac{a_{n,s,i}\gamma_i}{(E_i - E_n - \omega_s\eta_n)^2 + \gamma_i^2}|$ according to Eqs. (8) and (9). The quantity $E_i - E_n - \omega_s\eta_n$ in each denominator indicates the coupling of the ith quasiparticle with the nth state through the sth resonant mode of the system. A large contribution is expected when $E_i - E_n$ and $\omega_s\eta_n$ are very close to each other. If G_0 is used, then $E_i - \epsilon_n - \omega_s\eta_n$ will replace $E_i - E_n - \omega_s\eta_n$, which diminishes the underlying physics of the summation since the Kohn-Sham system is only an artificial noninteracting reference system, and the ϵ_n, energies of Kohn-Sham particles, do not have any clear physical meaning.

Second, the summation S_i is sensitive to the positions of the poles $E_n + \omega_s\eta_n$, which also requires the implementation of the self-consistency. For a given QP with energy E_i, simplifying E_n to ϵ_n changes the positions of the poles from $E_n + \omega_s\eta_n$ to $\epsilon_n + \omega_s\eta_n$. This only has a minor effect on $\mathrm{Re}\langle\psi_i|\Sigma_{xc}|\psi_i\rangle$, which is determined by the ensemble of the poles, including those lying far away from E_i. However, the simplification may cause considerable error to $|\mathrm{Im}\langle\psi_i|\Sigma_{xc}|\psi_i\rangle|$, which is mostly determined by the arrangement of the poles in the vicinity of E_i. The effect is illustrated schematically in Fig. 2, where unoccupied (occupied) energy levels ϵ_n obtained by DFT-LDA are shifted up (down) to yield the QP energy levels E_n. Yet the poles $\epsilon_n + \omega_s\eta_n$ are not moved together, leading to misplaced poles around a given energy level E_i, especially for the highest occupied molecular orbital (HOMO) and the lowest unoccupied molecular orbital (LUMO). In Fig. 2, the LUMO and HOMO QP energy levels are adjacent to some of the poles $\epsilon_n + \omega_s\eta_n$. This situation will not happen if the poles $E_n + \omega_s\eta_n$ are instead used since $E_n + \omega_s\eta_n$ will move together with E_n and maintain their relative positions correctly.

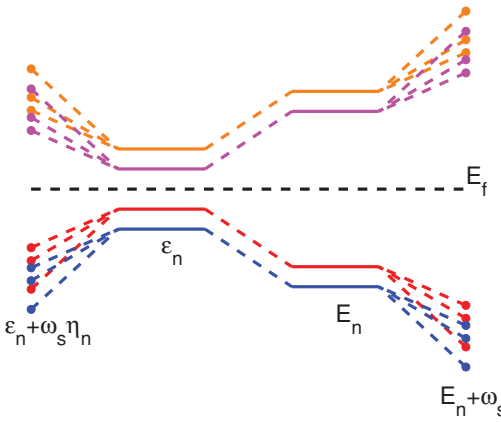

FIG. 2. (Color online) Schematic plot for the relation among LDA energies ϵ and hence derived poles $\epsilon_n + \omega_s\eta_n$ and QP energies E_n and hence derived poles $E_n + \omega_s\eta_n$. Each color defines a set including an energy level and poles accompanying the energy level. To maintain correct orders, E_n should be used together with $E_n + \omega_s\eta_n$. A mixture between E_n and $\epsilon_n + \omega_s\eta_n$ changes the pole arrangement in the vicinity of a QP energy level, which may introduce notable errors for the QP lifetime.

B. QP energies and lifetimes in Mg clusters

The QP energies and lifetimes of the HOMOs and LUMOs of the Mg_{10} and Mg_{40} simulated by both the GWA and the $GW\Gamma$ methods are listed in Table I. The results obtained without self-consistency are denoted by G_0. Eigenvalues from the LDA are also listed. When the decay rate of a QP is vanishingly small, its lifetime is denoted by ∞, indicating a rather long lifetime if only electron-electron inelastic scattering is considered. The relative effect of the self-consistency over the non-self-consistency on the QP energies can be readily read out from Table I. In general, the energy differences between the self-consistency and the non-self-consistency calculations are not very significant, especially for the larger cluster Mg_{40}, which is in accordance with our analysis about $\mathrm{Re}\langle\psi_i|\Sigma_{xc}|\psi_i\rangle$ in the previous paragraph.

On the other hand, the net effect of the self-consistency on the QP lifetimes is strongly size dependent. For Mg_{10}, no change has been observed in both the GWA and the $GW\Gamma$ calculations. However, the results have been qualitatively changed in the case of Mg_{40}. As discussed in Sec. III A, the QP lifetime is very sensitive to the poles in the vicinity of the QP energy. According to Fig. 2, the degree of the misplacement of the poles around the HOMO and LUMO can be roughly estimated by comparing the QP correction $|\Delta E_i| = |E_i - \epsilon_i|$ and the minimum frequency ω_1 of the reducible polarizability. The error of τ_i is insignificant when $|\Delta E_i|$ is smaller or comparable to ω_1, while it becomes significant when $|\Delta E_i|$ is larger than ω_1. This can be verified by comparing $|\Delta E_i|$ with ω_1, which are 1.50 (TDLDA) and 1.58 eV (RPA) for Mg_{10} and 0.27 (TDLDA) and 0.29 eV (RPA) for Mg_{40}.

Table I also illustrates the numerical difference between the two QP methods adopted in this paper. The net effect of the $GW\Gamma$ over the GWA is an upward energy shift, almost rigid for both the HOMO and LUMO. Furthermore, the upward energy shift is observed consistently for all occupied and unoccupied states, as shown in Fig. 3, where the energy levels of Mg_{40} obtained with the DFT-LDA, GWA, and $GW\Gamma$ methods are plotted. This energy shift, a feature of the $GW\Gamma$ method, has also been reported in bulk silicon,[24] as well as in a benzene molecule.[29] It can be explained using Eq. (8), where $GW\Gamma$ adds $2\langle\psi_i\psi_n|f_{xc}|\rho_s\rangle\langle\rho_s|V|\psi_i\psi_n\rangle$, a negative quantity, to each numerator and thus introduces unidirectional shifts to all E_n. Thomas *et al.* have measured the photoelectron spectra (PES) of Mg_n^- clusters.[34] The first PES peak of Mg_n^- can be used as a reference for the electronic affinity (EA) of Mg_n, neglecting the structural relaxation due to an extra electron. According to Ref. 34, EAs of Mg_{10} and Mg_{35} are about 1.70 and 2.85 eV, respectively. To compare with these data, we perform the calculations for the cluster Mg_{35}. EAs of Mg_{10} and Mg_{35} predicted by the $GW\Gamma$ are 1.49 and 2.71 eV, respectively, and those obtained by the GWA are 2.06 and 3.27 eV, respectively. We also test the basis completeness by increasing the size of the basis set for the simulation of

TABLE I. Calculated QP energies and lifetimes of the HOMOs and LUMOs of Mg_{10} and Mg_{40} clusters by the GWA and the $GW\Gamma$ methods with both self-consistency and non-self-consistency. The subscript in the first column stands for the number of Mg atoms in the cluster. DFT-LDA energies are also listed in the last column.

	G_0WA		GWA		$G_0W\Gamma$		$GW\Gamma$		DFT-LDA
	E (eV)	τ (fs)	E (eV)	τ (fs)	E (eV)	τ (fs)	E (eV)	τ (fs)	E (eV)
$HOMO_{10}$	−5.80	∞	−5.95	∞	−5.41	∞	−5.47	∞	−4.26
$LUMO_{10}$	−2.14	∞	−2.06	∞	−1.79	∞	−1.54	∞	−2.93
$HOMO_{40}$	−5.16	6.4	−5.31	∞	−4.73	16	−4.75	∞	−3.98
$LUMO_{40}$	−3.31	27	−3.35	∞	−2.89	12	−2.79	∞	−3.74

Mg_{10} and find that the number of bases is not the source of the uncertainty for EA of Mg_{10}.[35] Jellinek *et al.* have calculated the ionization potential (IP) of neutral magnesium clusters with gradient-corrected DFT.[36] IP of Mg_{10} is obtained as 5.5 eV in Ref. 36 and 5.47 eV ($GW\Gamma$) and 5.95 eV (GWA) in this work. Summarizing above, we find that the $GW\Gamma$ agrees with currently available data better than the GWA. Therefore our discussion will focus on the QP lifetimes in Mg_{40} obtained by the self-consistent $GW\Gamma$ approach.[37]

Inelastic lifetimes τ_i and scaled lifetimes $\tau_i|E_i - E_f|^2$ of hot electrons and holes in Mg_{40} calculated by the $GW\Gamma$ method are plotted versus the excitation energy $|E_i - E_f|$ in Figs. 4(a) and 4(b), respectively. The behavior of electrons in many bulk metals can be described as a free-electron gas (FEG). In a high-density FEG, lifetimes of hot electrons with low excitation energies follow an inverse quadratic law as derived by Quinn and Ferrell:[38]

$$\tau_i^{\mathrm{QF}} = 263 r_s^{-5/2}(E_i - E_F)^{-2}\ \mathrm{eV}^2\ \mathrm{fs}. \qquad (11)$$

This is equivalent to a constant scaled lifetime $\tau_i|E_i - E_f|^2$ for all hot electrons, which is 22.8 fs eV^2 for bulk magnesium with $r_s = 2.66$. However, in the cluster Mg_{40}, scaled QP lifetimes with low excitation energies ($|E_i - E_f| < 2.1$ eV) are longer than the lifetime obtained from Eq. (11) and are energy dependent. On the other hand, the pattern of scaled QP lifetimes with high excitation ($|E_i - E_f| \geqslant 2.1$ eV) are relatively flat. Thus the results indicate that there are two energy regimes, as illustrated in Fig. 4: a low-energy regime (R_{LE}) and a high energy one (R_{HE}), which will be discussed separately.

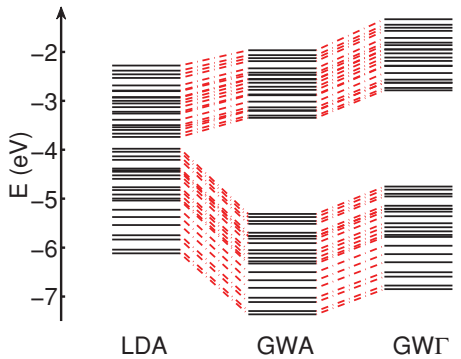

FIG. 3. (Color online) Energy levels of Mg_{40} calculated by the LDA, GWA, and $GW\Gamma$ methods. The net effect of the $GW\Gamma$ over the GWA method is an almost rigid upward shift.

As a general trend, the scaled QP lifetimes in the R_{LE} increase with decreasing $|E_i - E_f|$ and become notably longer than τ^{QF}. This is qualitatively different from the result obtained in the bulk magnesium.[39] The latter shows that the inelastic lifetimes of electrons with low excitation energies are close to (or shorter than) τ^{QF}. It has been noted that the QP scattering rate is determined by two competing factors: the number of states for possible transitions of a hot electron and the dynamical screening to the interaction between this hot electron and other electrons.[6] As shown in Fig. 3, energy states of a small metallic cluster such as Mg_{40} are missing around the Fermi level due to the confinement of the electrons, which is quite different from the bulk counterpart. This reduces the number of states available for transitions of all hot electrons (holes) in a cluster. The effect becomes dominant for those energy levels in the R_{LE} with low excitation energies and thus leads to relatively long QP lifetimes, and the lower the excitation energy is, the longer the lifetime is. Also, in the R_{LE} we find that the lifetimes of hot electrons and hot holes with the

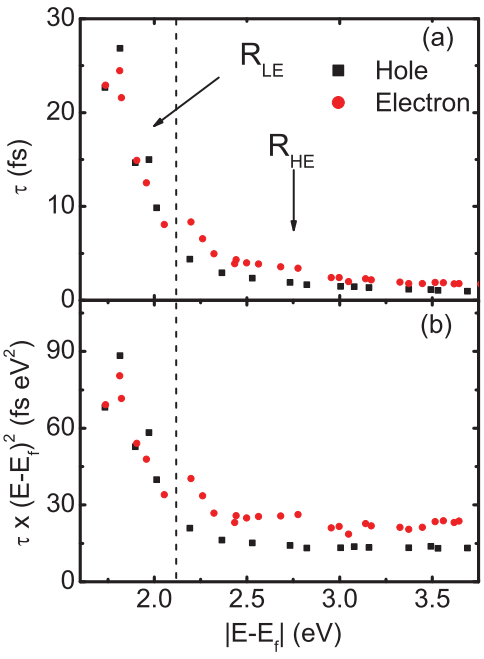

FIG. 4. (Color online) (a) QP lifetimes and (b) scaled QP lifetimes in Mg_{40} obtained with the self-consistent $GW\Gamma$ approach. The vertical dashed line separates both plots into a low-energy regime (R_{LE}) and a high-energy regime (R_{HE}).

same $|E_i - E_f|$ are close to each other, which is similar to the results obtained from the FEG in the low-excitation regime.[38]

In the R_{HE}, the scaled lifetimes of hot electrons fluctuate in the range of 21–24 fs eV^2 with increasing $|E_i - E_f|$, which is quite close to 22.8 fs eV^2 calculated from Eq. (11). In the bulk Mg, the scaled lifetimes in the same energy regime increase from 25 to 30 fs eV^2 with increasing excitation energy.[39] It is speculated that the slight difference between the cluster and the bulk could be attributed to the electronic spill effect, as the electron wave functions can stretch outside of a finite-potential well. This effect is notable for small metallic clusters[40] and leads to lower electron densities and thus shorter QP lifetimes.

Note that our results here are different from those in Ref. 21, where shorter lifetimes are found based on spherical jellium model calculations. The difference could be attributed to the definition of the QP excitation energy. In Ref. 21, it is defined as $|\epsilon_i - \epsilon_f|$, while for the nanoclusters in this article, it is defined as $|E_i - E_f|$, which can be approximated as $|E_i - \epsilon_i| + |\epsilon_i - \epsilon_f|$. The GW correction term $|E_i - \epsilon_i|$ vanishes in infinite uniform electron gas, yet it could be a large number in finite systems and also strongly size dependent, as can be seen in Table I.

The scaled lifetimes of hot holes in the R_{HE} decrease slowly with increasing $|E_i - E_f|$. They are shorter than those of hot electrons with the same $|E_i - E_f|$, which also has been found in the case of the FEG.[6] In a finite system such as Mg_{40}, the shorter hole lifetimes can be attributed to the smaller angular momentums of these holes, which leads to more possible transitions than electrons. This is an analogy to the bulk, where we can attribute shorter hole lifetimes to the smaller momentums of holes.[41] Note that in simple s-p systems, there are no localized d electrons. Correspondingly, we have not observed any localized d holes with longer lifetimes than those of electrons, as has been demonstrated in noble metals.[41,42]

IV. CONCLUSION

We calculate the QP energies and lifetimes in Mg_{10} and Mg_{40} clusters and demonstrate the necessity of using self-consistency for the calculations of the QP lifetimes in finite systems. For Mg_{40}, the lifetimes of QPs near the HOMO and LUMO are found to be longer than those in a FEG with the same valence electron density as in bulk Mg due to the lack of states available for transitions. In the high-excitation-energy regime, scaled lifetimes of hot electrons converge to the range of 21–24 fs eV^2, consistent with the value (22.8 fs eV^2) predicted by the inverse quadratic relation of Quinn and Ferrell. In this regime, hot holes exhibit shorter lifetimes compared with hot electrons due to the smaller angular momentums of holes.

ACKNOWLEDGMENT

This project is sponsored by the National Science Foundation (Grant No. CTS-0500402/CBET-0830098).

*tzeng2@mit.edu

[1] H. Petek and S. Ogawa, Prog. Surf. Sci. **56**, 239 (1997).
[2] J. Bokor, Science **246**, 1130 (1989).
[3] E. Knoesel, A. Hotzel, and M. Wolf, Phys. Rev. B **57**, 12812 (1998).
[4] L. Bürgi, O. Jeandupeux, H. Brune, and K. Kern, Phys. Rev. Lett. **82**, 4516 (1999).
[5] R. Knorren, K. H. Bennemann, R. Burgermeister, and M. Aeschlimann, Phys. Rev. B **61**, 9427 (2000).
[6] P. M. Echenique, J. M. Pitarke, E. V. Chulkov, and A. Rubio, Chem. Phys. **251**, 1 (2000).
[7] E. V. Chulkov, A. G. Borisov, J. P. Gauyacq, D. Sánchez-Portal, V. M. Silkin, V. P. Zhukov, and P. M. Echenique, Chem. Rev. **106**, 415 (2006).
[8] W. A. de Heer, Rev. Mod. Phys. **65**, 611 (1993).
[9] K. K. Likharev, Proc. IEEE **87**, 606 (1999).
[10] K. Watanabe, D. Menzel, N. Nilius, and H. J. Freund, Chem. Rev. **106**, 4301 (2006).
[11] C. Voisin, D. Christofilos, N. Del Fatti, F. Vallée, B. Prével, E. Cottancin, J. Lermé, M. Pellarin, and M. Broyer, Phys. Rev. Lett. **85**, 2200 (2000).
[12] M. Merschdorf, C. Kennerknecht, and W. Pfeiffer, Phys. Rev. B **70**, 193401 (2004).
[13] N. Pontius, P. S. Bechthold, M. Neeb, and W. Eberhardt, Phys. Rev. Lett. **84**, 1132 (2000).
[14] Y. D. Kim, M. Niemietz, P. Gerhart, F. v. Gynz-Rekowski, and G. Ganteför, Phys. Rev. B **70**, 035421 (2004).
[15] A. E. Bragg, J. R. R. Verlet, A. Kammrath, O. Cheshnovsky, and D. M. Neumark, J. Chem. Phys. **122**, 054314 (2005).
[16] J. Stanzel, F. Burmeister, M. Neeb, and W. Eberhardt, J. Chem. Phys. **127**, 164312 (2007).
[17] M. S. Hybertsen and S. G. Louie, Phys. Rev. B **34**, 5390 (1986).
[18] R. W. Godby, M. Schlüter, and L. J. Sham, Phys. Rev. B **37**, 10159 (1988).
[19] I. Campillo, J. M. Pitarke, A. Rubio, E. Zarate, and P. M. Echenique, Phys. Rev. Lett. **83**, 2230 (1999).
[20] G. Onida, L. Reining, and A. Rubio, Rev. Mod. Phys. **74**, 601 (2002).
[21] M. Quijada, R. Díez Muiño, A. G. Borisov, J. A. Alonso, and P. M. Echenique, New J. Phys. **12**, 053023 (2010).
[22] G. D. Mahan, *Many-Particle Physics*, 3rd ed. (Kluwer/Plenum, New York, 2000).
[23] L. Hedin, Phys. Rev. **139**, A796 (1965).
[24] R. Del Sole, L. Reining, and R. W. Godby, Phys. Rev. B **49**, 8024 (1994).
[25] W. G. Aulbur, L. Jönsson, and J. W. Wilkins, in *Solid State Physics*, edited by F. Seitz, D. Turnbull, and H. Ehrenreich (Academic, New York, 2000), Vol. 54, p. 1.
[26] F. Aryasetiawan and O. Gunnarsson, Rep. Prog. Phys. **61**, 237 (1998).
[27] M. Rohlfing and S. G. Louie, Phys. Rev. B **62**, 4927 (2000).

[28]M. E. Casida, in *Recent Advances in Density-Functional Methods, Part I*, edited by D. P. Chong (World Scientific, Singapore, 1995), p. 155.
[29]M. L. Tiago and J. R. Chelikowsky, Phys. Rev. B **73**, 205334 (2006).
[30]J. M. Soler, E. Artacho, J. D. Gale, A. García, J. Junquera, P. Ordejón, and D. Sánchez-Portal, J. Phys. Condens. Matter **14**, 2745 (2002).
[31]N. Troullier and J. L. Martins, Phys. Rev. B **43**, 1993 (1991).
[32]U. Trottenberg, C. W. Oosterlee, and A. Schüller, *Multigrid* (Academic, San Diego, 2001).
[33]B. Holm and U. von Barth, Phys. Rev. B **57**, 2108 (1998).
[34]O. C. Thomas, W. J. Zheng, S. J. Xu, and K. H. Bowen, Phys. Rev. Lett. **89**, 213403 (2002).
[35]The IP of Mg_{10} obtained by the $GW\Gamma$ with the basis set 4Z4P is 1.45 eV, which is slightly lower than that of the DZP result (1.49 eV).
[36]J. Jellinek and P. H. Acioli, J. Phys. Chem. A **106**, 10919 (2002).
[37]Mg_{40} is more illustrative due to more energy states.
[38]J. J. Quinn and R. A. Ferrell, Phys. Rev. **112**, 812 (1958).
[39]I. Campillo, V. M. Silkin, J. M. Pitarke, E. V. Chulkov, A. Rubio, and P. M. Echenique, Phys. Rev. B **61**, 13484 (2000).
[40]W. Ekardt, Phys. Rev. B **29**, 1558 (1984).
[41]I. Campillo, A. Rubio, J. M. Pitarke, A. Goldmann, and P. M. Echenique, Phys. Rev. Lett. **85**, 3241 (2000).
[42]Z. J. Yi, Y. C. Ma, M. Rohlfing, V. M. Silkin, and E. V. Chulkov, Phys. Rev. B **81**, 125125 (2010).